Turkish Journal of Electrical Engineering & Computer Sciences

http://journals.tubitak.gov.tr/elektrik/

Research Article

Turk J Elec Eng & Comp Sci
(2018) 26: 1771 – 1782

doi:10.3906/elk-1710-200

A novel model for minimizing unnecessary handover in heterogeneous networks

Babatunji OMONIWA[1,*], Riaz HUSSAIN[2], Junaid AHMED[2], Adeel IQBAL[2], Ahmed MURKAZ[3], Qadeer UL-HASAN[2], Shahzad Ali MALIK[2]

[1]Computer Science Programme, National Mathematical Centre, Abuja, Nigeria
[2]Department of Electrical Engineering, COMSATS Institute of Information Technology, Islamabad, Pakistan
[3]Engineering Department, Stonefly Inc., Hayward, CA, USA

Received: 21.10.2017 • **Accepted/Published Online:** 09.05.2018 • **Final Version:** 27.07.2018

Abstract: Over the years, vertical handover necessity estimation has attracted the interest of numerous researchers. Despite the attractive benefits of integrating different wireless platforms, mobile users are confronted with the issue of detrimental handover. This paper uses extensive geometric and probabilistic techniques to develop a realistic and novel model for the coverage area of a wireless local area network (WLAN) cell with an aim to minimize unnecessary handover and handover failure of a mobile node (MN) traversing the WLAN cell from a third-generation network. The dwell time is estimated along with the threshold values to ensure an optimal handover decision by the MN, while the probability of unnecessary handover and probability of handover failure are kept within tolerable bounds. Monte Carlo simulations were carried out to assess the behavior of the proposed and existing models. Simulation results showed that our proposed model is more robust and capable of keeping unnecessary handover probability and handover failure probability closest to a predefined probability benchmark. For model validation, the Nash–Sutcliffe coefficient was used to compute the efficiency of the proposed model, which achieved a value of 98.82% indicating the accuracy of the model.

Key words: Vertical handover necessity estimation, unnecessary handover, handover failure, probabilistic model

1. Introduction

With the rapid growth in the use of the Internet and wireless services, the challenge to support generalized mobility and provision of ubiquitous services to users while integrating diverse access technologies (GSM, 3G, 4G, WLAN, WiMAX, and Bluetooth) has attracted research attention. Due to increased demand for mobile data, users now require access networks that use multiple layers (macro- as well as microcells) and multiple technologies to meet growing needs. Vertical handover implies handover from/to different technologies, like from cellular into 802.11 and vice versa. As a mobile node (MN) moves within a heterogeneous environment, satisfactory quality of service (QoS) is desired by ensuring efficient vertical handover.

Vertical handover can be defined as when an MN moves from one access network to another while maintaining the live call or session. In contrast to horizontal handovers, vertical handovers can be instigated for convenience rather than connectivity purposes only. As such, the choice to perform vertical handover may depend on factors such as available bandwidth, received signal strength (RSS), access cost, dwell time, security, and speed [1–6]. For optimal decision making, it is imperative to weigh the benefits against the detriments

*Correspondence: tunjiomoniwa@gmail.com

before initiating a vertical handover. Existing schemes use the regular-shaped coverage region for modeling, which is not a real-world scenario, as the actual coverage region is irregular in shape.

The focus of this paper is to introduce an amoebic-based geometric model that extends the ideal circular coverage model employed in previous works. We build upon the RSS-based dwell time approach, which is easy to implement; however, these algorithms are seriously limited by slow fading [7,8]. Slow fading can be caused by events such as shadowing, where a large obstruction such as a hill or large building obscures the main signal path between the transmitter and the receiver. Previous works assume the coverage area of the WLAN cell to be perfectly circular. The motivation of this work is to extend previous works on handover necessity estimation (HNE). This paper presents a novel and realistic model that depicts the actual behavior of a WLAN coverage area. As such, we consider the effects of slow fading in our simulations. The proposed model will ensure an efficient minimization of the probability of unnecessary handover and handover failure for an MN traversing a realistic WLAN cell from a 3G network by the following factors:

- The WLAN cell shape is not exactly circular, but irregular.
- The cell shape changes with changes in nature of obstruction at different instances, humidity, temperature, etc.

2. State of the art

Related works on vertical handover can be grouped into three types [5], the RSS-based, cost-based, and other related works, which are briefly described.

RSS-based related works: Several RSS-based handover algorithms have been developed for wireless communications. A linear approximation of the traveled distance was proposed in [1] to minimize the probability of unnecessary handover. A traveling distance prediction based handover decision method was proposed in [2], and a dwell time prediction model was presented in [3]. A novel algorithm was developed using the concept of dynamic boundary area to support seamless vertical handover between 3G and WLAN in [4]. However, the geometric models considered were not of a realistic coverage cell shape.

Cost-based related works: Handover cost is a function of the available bandwidth, security, power consumption, and the monetary cost [9]. As the need for voice and video services rises, available bandwidth, power consumption, security, etc. will be a major factor used to indicate network conditions to trigger handovers. In [10], available bandwidth and monetary cost were used as metrics for handover decisions. Cost-based algorithms are usually complex, as they require collecting and normalization of different network metrics.

Other related works: An analytical framework to evaluate vertical handover algorithms with new extensions for traditional hysteresis-based and dwell-timer–based algorithms was proposed in [11]. Using a probability approach, [6] worked on the assessment of wrong decision probability, which assures a trade-off between network performance maximization and mitigation of the ping-pong effect. An algorithm was proposed in [12] that allows multimode mobile terminals to select and associate with the network access point (AP) to minimize the average overall power consumption at the MN and guarantee minimum supported QoS for on-going connections. The proposed algorithm was able to reduce the vertical handover frequency and keep the received bits as high as possible. The work in [13] proposed an algorithm that predicts the resource requirements regarding the mobility of their users and prioritizes handoff calls over incoming calls. In [14], a fuzzy-logic–based model was proposed to perform a handover in case of degraded QoS. The technique was able to perform efficient HNE.

3. Amoebic wireless coverage concept

Both theoretical and empirical propagation models show that average received signal power decreases logarithmically with distance[1]. A number of factors, apart from the frequency and the distance, influence losses encountered by propagated signals from the AP to the MN. In order to accurately model a wireless coverage area, these factors must be considered.

The factors include:

- the height of the MN antenna;
- the height of the AP relative to the surrounding terrain;
- the terrain irregularity (undulation or roughness);
- the land usage in the surroundings of MN: urban, suburban, rural, open, etc.

Due to these combined effects, this paper presents an amoebic WLAN cell that gives a realistic representation of the wireless coverage with a perspective of the shadowing concept. There are three different rates of variation for wireless signals as it propagates away from the AP. We have the very slow variation, called path loss, which is a function of the distance between the AP and MN. Then we have slow variation, which results from shadowing effects. Finally, we have fast variation, due to multipath. Signal variations caused by multipath, in the case where the direct signal is assumed to be totally blocked, are usually represented by a Rayleigh distribution. The slow variability of the received signal, which is due to shadowing, is usually assumed to follow a log-normal distribution [15].

This paper considers the effect of the path loss and shadowing. The effect of multipath is neglected and beyond the scope of this work. Figure 1a gives a clearer picture of the behavior of wireless signals in a coverage area with different coverage probabilities. Figure 1b shows 50% coverage and Figure 1c shows 80% coverage of the MN, with instances where it experiences poor signal strength. These slow signal deviations due to shadowing follow a Gaussian distribution and are given as

$$f(r) = \frac{1}{\sigma\sqrt{2\pi}} \exp\left(\frac{-(r-\mu)^2}{2\sigma^2}\right), \tag{1}$$

where μ is the mean value and σ^2 is the variance of the Gaussian random variable r.

Suppose we have the radius of the WLAN cell, which is a continuous random variable R with probability distribution function (PDF) $f(r)$, as shown in Eq. (1), and we want to evaluate the expectation E[g(R)] for some function $g(r)$. This entails evaluating the integral

$$E[g(R)] = \int_{-\infty}^{\infty} f(r)\, g(r)\, dr \tag{2}$$

Since the integral is not easily tractable by analytical or standard numerical methods, the study approached it by simulating realizations of $r_1, r_2, r_3, ...r_n$ of R, and since the variance is finite, we apply the law of large numbers to obtain an approximation [16].

$$E[g(R)] \sim \frac{1}{n} \sum_{i=1}^{n} g_i(r) \tag{3}$$

The expression in Eq. (3) gives justification for the Monte Carlo simulation carried out in the previous study.

[1] $PL(d)_{dB} = P(\text{transmitted})_{dB} - P(\text{received})_{dB} = PL(d_0) + 10\beta\log(d = d_0) + R_\sigma$, where R_σ is the Gaussian random variable with standard deviation, σ, and β is the path loss exponent.

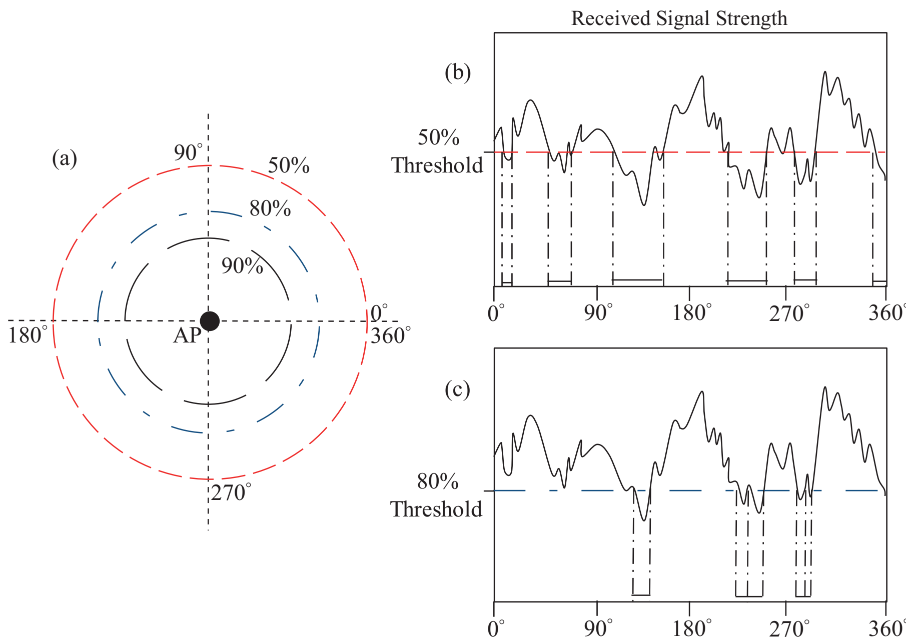

Figure 1. (a) Coverage regions for 50%, 80%, and 90%. (b) Received signal strength (RSS) while moving along the 50% contour. (c) RSS while moving along the 80% contour.

4. Proposed scheme

We present an amoebic-based model that extends the ideal circle model employed in previous works [1–4]. The work assumes that when an MN is in the coverage area of its present access network, adjacent to a WLAN cell, it may enter the boundary area of the WLAN cell at any point, P_A, and move along the path $|P_A P_D|$, exiting from any point, P_D, on the coverage boundary (as shown in Figure 2). We further assume that the speed, v, of the MN has a bound of $[v_{min}, v_{max}]$, and the direction of motion, θ, is uniformly distributed in $[0, \pi]$, while [2] and [3] with an angle of arrival were considered in the previous works. The cell radius is assumed to be stochastic and normally (Gaussian) distributed with defined mean and variance. The justification for having a normal distribution can be given in terms of the central limit theorem [16], as the total attenuation experienced in a wireless link results from the tallying of several individual shadowing processes forming a Gaussian distribution.

The angle of arrival Θ_A and angle of departure Θ_D are assumed to be uniformly distributed within the bound of Θ and we express the angle between random positions of P_A and P_D as $\Theta = |\Theta_D - \Theta_A|$.

A realistic coverage area of the WLAN cell with an amoebic structure is considered in this work. As there is only a possibility that the MN moves in and out of the coverage area in any half section of Figure 2, we therefore derive an expression to calculate the PDF of θ. The PDF of the arrival and departure of the MN from the WLAN coverage at the points P_A and P_D, respectively, is given by

$$f_{\Theta A}(\theta_A) = \begin{cases} \frac{1}{\pi}, & 0 \leq \theta_A \leq \pi, \\ 0, & otherwise. \end{cases} \tag{4}$$

$$f_{\Theta D}(\theta_D) = \begin{cases} \frac{1}{\pi}, & 0 \leq \theta_D \leq \pi, \\ 0, & otherwise. \end{cases} \tag{5}$$

Since the arrival and departure points of the mobile nodes are independent, the joint PDF is therefore given as

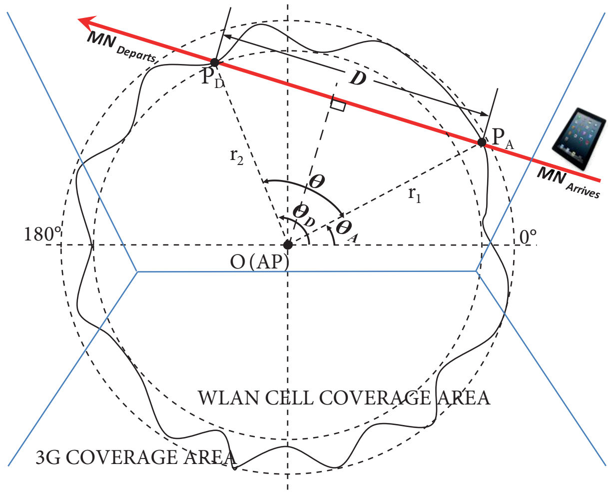

Figure 2. A mobile node entering an amoebic WLAN coverage area.

the product of their individual marginal functions.

$$f_{\Theta A,\,\Theta D}\,(\theta_A,\,\theta_D) \;=\; \begin{cases} \frac{1}{\pi^2}, & 0 \,\le\, \theta_A,\,\theta_D \,\le\, \pi, \\ 0, & otherwise. \end{cases} \tag{6}$$

To obtain the probability of $\Theta \le \theta$, we find the cumulative distribution function (CDF) of Θ by

$$F_\Theta(\theta) \;=\; P(\Theta \;\le\; \theta)$$

$$= \int \int_\epsilon f_{\Theta A,\,\Theta D}(\theta_A,\,\theta_D)\; d\theta_D\; d\theta_A, \tag{7}$$

where ϵ is a set of arrival and departure points by the MN, such that $\Theta \le \theta$ and $0 \le \Theta \le \pi$, $P(\Theta \le \theta) = 0$ for $\Theta < 0$ and $P(\Theta \le \theta) = 1$ for $\Theta > \pi$ [2]. From Figure 2, Eq. (7) can be expressed as

$$F_\Theta(\theta) \;=\; \frac{1}{\pi^2}\left(\int_0^{\theta}\int_0^{\theta\,+\,\theta_D} d\theta_A\; d\theta_D \;+\; \int_{\theta}^{\pi\,-\,\theta}\int_{\theta_D\,-\,\theta}^{\theta_D\,+\,\theta} d\theta_A\; d\theta_D \;+\; \int_{\pi\,-\,\theta}^{\pi}\int_{\theta_D\,-\,\theta}^{\pi} d\theta_A\; d\theta_D\right) \tag{8}$$

$$F_\Theta(\theta) \;=\; \frac{(2\,\pi\;-\;\theta)\;\theta}{\pi^2},\; 0\;\le\;\theta\;\le\;\pi \tag{9}$$

When we take the derivative of the CDF in Eq. (9), we obtain the PDF of θ and this is given by

$$f_\Theta(\theta) \;=\; \begin{cases} \frac{2\,(\pi\,-\,\theta)}{\pi^2}, & 0 \;\le\; \theta \;\le\; \pi, \\ 0, & otherwise \end{cases} \tag{10}$$

We can now use the PDF of θ to compute the PDF of the traversing time of the mobile node, t_{WLAN}. Using the cosine formula, we formulate a geometric expression of the traversing distance, D, from Figure 2.

$$D \;=\; \sqrt{r_{d1}^2 \;+\; r_{d2}^2 \;-\; 2\,r_{d1}\,r_{d2}\;\cos\theta} \tag{11}$$

The traversal time within the WLAN cell depends on the traversing angle, and it is expressed as

$$t_{WLAN} = g(\theta)$$

$$= \frac{\sqrt{r_{d1}^2 + r_{d2}^2 - 2\, r_{d1}\, r_{d2}\, \cos\theta}}{v} \quad (12)$$

The PDF of the traversing time can thus be expressed as [17]

$$f_T(t) = \sum_{i=1}^{n} \left| \frac{f(\theta_i)}{g'(\theta_i)} \right|_{\theta_i}, \quad (13)$$

where θ is the root of the function $g(\theta)$, and $g\prime(\theta)$ is the derivative of $g(\theta)$

$$\theta = \arccos\left(\frac{r_{d1}^2 + r_{d2}^2 - t_{WLAN}^2\, v^2}{2\, r_{d1}\, r_{d2}} \right) \quad (14)$$

We have the derivative of $g(\theta)$ as

$$g'(\theta) = \frac{r_{d1}\, r_{d2}\, \sin\theta}{v\sqrt{r_{d1}^2 + r_{d2}^2 - 2\, r_{d1}\, r_{d2}\, \cos\theta}} \quad (15)$$

Thus, substituting Eq. (14) into Eq. (15) yields

$$g'(\theta) = \frac{r_{d1}\, r_{d2}\, \sin\left(\arccos\left(\frac{r_{d1}^2 + r_{d2}^2 - t_{WLAN}^2\, v^2}{2\, r_{d1}\, r_{d2}}\right)\right)}{v\sqrt{r_{d1}^2 + r_{d2}^2 - 2\, r_{d1}\, r_{d2}\, \cos\left(\arccos\left(\frac{r_{d1}^2 + r_{d2}^2 - t_{WLAN}^2\, v^2}{2\, r_{d1}\, r_{d2}}\right)\right)}}$$

$$= \frac{\sqrt{4\, r_{d1}^2\, r_{d2}^2 - (r_{d1}^2 + r_{d2}^2 - t_{WLAN}^2\, v^2)^2}}{2\, t_{WLAN}\, v^2} \quad (16)$$

To obtain the PDF at θ, we substitute Eq. (14) into Eq. (10).

$$f_\Theta(\theta) = \frac{2\left(\pi - \arccos\left(\frac{r_{d1}^2 + r_{d2}^2 - t_{WLAN}^2\, v^2}{2\, r_{d1}\, r_{d2}}\right)\right)}{\pi^2} \quad (17)$$

Thus, from Eqs. (16) and (17), we can now obtain the PDF of the traversal time by using Eq. (13).

$$f_T(t) = \frac{4\, v^2\, t_{WLAN}\left(\pi - \arccos\left(\frac{r_{d1}^2 + r_{d2}^2 - t_{WLAN}^2\, v^2}{2\, r_{d1}\, r_{d2}}\right)\right)}{\pi^2\sqrt{4\, r_{d1}^2\, r_{d2}^2 - (r_{d1}^2 + r_{d2}^2 - t_{WLAN}^2\, v^2)^2}} \quad (18)$$

5. Handover decisions

To keep unnecessary handover and handover failure within satisfactory bounds, it is imperative to find two time threshold values, M and N, which are used for handover decisions. Table 1 shows the algorithm of how handover decisions are made using the proposed HNE scheme. The vertical handover decision scheme presented in this manuscript can be readily integrated into the IEEE 802.21 media-independent handover framework, since it aims to support seamless roaming among a variety of wireless access network technologies.

Table 1. Handover decision algorithm using the proposed HNE scheme.

Algorithm for Handover Decision using the Proposed HNE Scheme
MN traverses a Heterogeneous Wireless Environment
While MN is in PresentAccessNetwork:
MN scans for available AccessNetwork
If WLAN is Available
Begin Handover Necessity Estimation
//MN estimates the traversal time, t_{WLAN}
//MN computes time threshold values, M & N,
//from Eq. (23) & Eq. (28), respectively.
If t_{WLAN} > time threshold, *M & N*
Initiate the Handover Procedure to the WLAN
Else
Maintain the On-going Connection
End If
Else
MN remains in its PresentAccessNetwork
End If
End While

5.1. Probability of handover failure

Handover failure is said to occur if the handover time (τ_A) into the WLAN cell exceeds the overall time spent by the mobile node in the WLAN coverage area [3]. A time threshold, M, is defined and the probability of handover failure is kept within desirable bounds. We now use the PDF of traversal time obtained in Eq. (18) to derive an expression for the CDF of the probability of handover failure, P_f.

$$P_f = \begin{cases} P\left[M < T \le \tau_A\right], & 0 \le T \le \frac{(r_{d1}+r_{d2})}{v}, \\ 0, & Otherwise. \end{cases} \tag{19}$$

$$P\left[M < T \le \tau_A\right] = \int_M^{\tau_A} f_T(t)\, dt \tag{20}$$

P_f is expressed as

$$P_f = \frac{\left(2\pi - \arccos\left(\frac{r_{d1}^2 + r_{d2}^2 - \tau_A^2 v^2}{2 r_{d1} r_{d2}}\right)\right) \arccos\left(\frac{r_{d1}^2 + r_{d2}^2 - \tau_A^2 v^2}{2 r_{d1} r_{d2}}\right)}{\pi^2}$$

$$- \frac{\left(2\pi - \arccos\left(\frac{r_{d1}^2 + r_{d2}^2 - M^2 v^2}{2 r_{d1} r_{d2}}\right)\right) \arccos\left(\frac{r_{d1}^2 + r_{d2}^2 - M^2 v^2}{2 r_{d1} r_{d2}}\right)}{\pi^2} \tag{21}$$

$$q = \pi \pm \sqrt{\pi^2 \ (1 + P_f) - 2\pi z + z^2} \tag{22}$$

Hence, we find the time threshold for handover failure, M,

$$M = \frac{\sqrt{r_{d1}^2 + r_{d2}^2 - 2 r_{d1} r_{d2} \cos(q)}}{v} \tag{23}$$

5.2. Probability of unnecessary handover

This work attempts to minimize the number of unnecessary handovers. This is achieved by calculating the time threshold value, N. An unnecessary handover is said to occur when the traversing time of a mobile node in a WLAN cell is smaller than the sum of the handover time into (τ_A) and out of (τ_D) the WLAN coverage area [3]. Given that $\tau_T = \tau_A + \tau_D$, we now use the PDF of traversal time obtained in Eq. (18) to derive an expression for the CDF of the probability of unnecessary handover, P_u. This is shown in Eq. (26).

$$P_u = \begin{cases} P\,[N < T \leq \tau_T], & 0 \leq T \leq \frac{(r_{d1} + r_{d2})}{v}, \\ 0, & Otherwise. \end{cases} \tag{24}$$

$$P_u = P\,[N < T \leq \tau_T] = \int_N^{\tau_T} f_T(t)\ dt \tag{25}$$

P_u is expressed as

$$P_u = \frac{\left(2\pi - \arccos\left(\frac{r_{d1}^2 + r_{d2}^2 - \tau_T^2 v^2}{2 r_{d1} r_{d2}}\right)\right) \arccos\left(\frac{r_{d1}^2 + r_{d2}^2 - \tau_T^2 v^2}{2 r_{d1} r_{d2}}\right)}{\pi^2}$$

$$- \frac{\left(2\pi - \arccos\left(\frac{r_{d1}^2 + r_{d2}^2 - N^2 v^2}{2 r_{d1} r_{d2}}\right)\right) \arccos\left(\frac{r_{d1}^2 + r_{d2}^2 - N^2 v^2}{2 r_{d1} r_{d2}}\right)}{\pi^2} \tag{26}$$

Let $z = \arccos\left(\frac{r_{d1}^2 + r_{d2}^2 - \tau_T^2 v^2}{2 r_{d1} r_{d2}}\right)$. We obtain the following expression for N, which is a function of handover latency, velocity, stochastic coverage radius, and probability of unnecessary handover.

$$y = \pi \pm \sqrt{\pi^2 \ (1 + P_u) - 2\pi z + z^2} \tag{27}$$

Now we get a new expression for time threshold for unnecessary handover[2], N,

$$N = \frac{\sqrt{r_{d1}^2 + r_{d2}^2 - 2 r_{d1} r_{d2} \cos(y)}}{v} \tag{28}$$

In this section, we have obtained new expressions of time threshold values, M and N.

[2] Yan et al. [2] arrived at a time threshold, $t_{WLAN} = \frac{2R}{v} \sin\left(\arcsin\left(\frac{v\tau}{2R} - \frac{\pi}{2} P\right)\right)$, and Hussain et al. [3] arrived at $t_{WLAN} = \frac{2Rk}{v\sqrt{1+k^2}}$, where $k = \tan\left(\arctan\left(\frac{v\tau}{\sqrt{4R^2 - v^2\tau^2}}\right) - \frac{P\pi}{2}\right)$.

5.3. Results

For the experiments, we used threshold values, M and N, obtained in Eqs. (23) and (28), respectively. We assumed that the transversal angle, θ, falls within $[0, \pi]$ bound. We also used dwell time, T, obtained in Eq. (12). Benchmark values for both P_u and P_f were set to 0.01 and the handover latencies from 3G to the WLAN and from the WLAN to the 3G network as 1 s. In this work, only the shadowing effect was considered and the WLAN radius was simulated to be random with a fixed mean of 50 m and a random variation of [–2, +2] to depict fading, implying that the WLAN radius falls within 48–52 m range. We carried out simulations using MATLAB. Due to the stochastic behavior resulting from the random (amoebic) geometry of the WLAN coverage area during the simulations, the probability values changed over each iteration. As such, Monte Carlo simulations were then carried out using one million iterations to precisely determine the effect of mobility on handover probabilities. Our proposed model was simulated along with other state-of-the-art time prediction vertical handover models [1–4] and the performance can be seen in Figures 3 and 4. Simulation results obtained using our proposed model outperformed previous models of unrealistic geometry. From the results obtained, we see that P_u and P_f increase with a corresponding increase in the velocity of the mobile node. This confirms that speed has a direct impact on the handover probabilities, as observed in previous works [1–4]. This implies that there is a higher tendency for connection breakdown when the MN moves very fast.

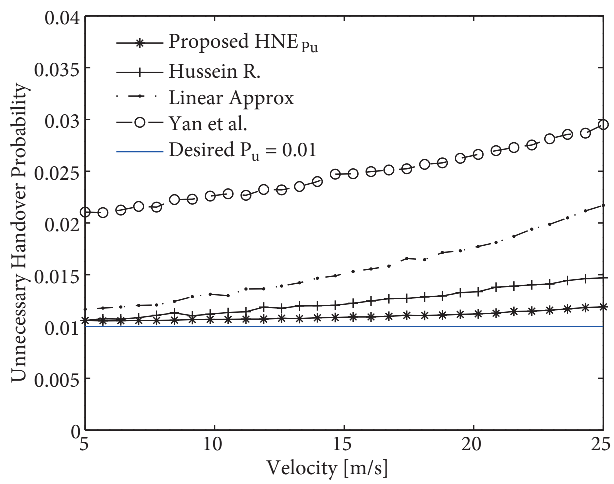

Figure 3. P_u versus velocity of the MN.

Generally, results show that the proposed model outperforms Hussain's linear approximation method employed in [1], Yan et al. [2], and Hussain et al. [3], all of which considered a circular coverage cell. Our proposed model keeps both P_u and P_f close to the predefined probability benchmark of 0.01 for the entire velocity range considered. In addition, our work considered the effect of slow fading and presents a realistic depiction of the WLAN coverage area, giving a true picture of the stochastic wireless environment.

The time threshold parameter, M, is dependent on the velocity of the MN. As such, we show the impact of the velocity on the time threshold parameter, M. From Figure 5, we can see that the MN computes its time threshold based on its average velocity. At a lower velocity, the MN has a higher threshold value. This implies that the MN is given more time to make a handover decision to its desired access network. We also observe that, at different values of P_f, M only adapts to the change in velocity of the MN.

The overlapping plots in Figure 5 show that P_f has no impact on the time threshold value and it only

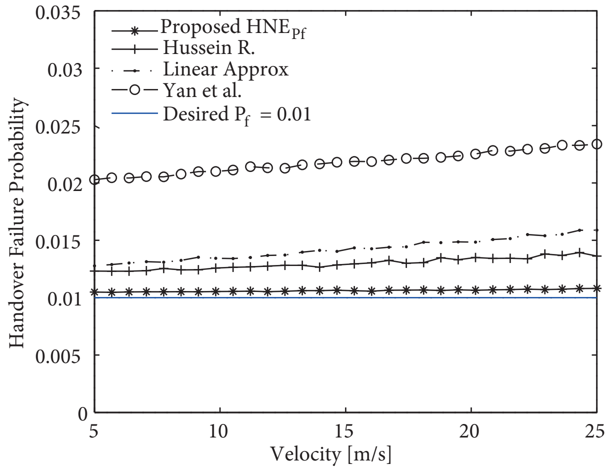

Figure 4. P_f versus velocity of the MN.

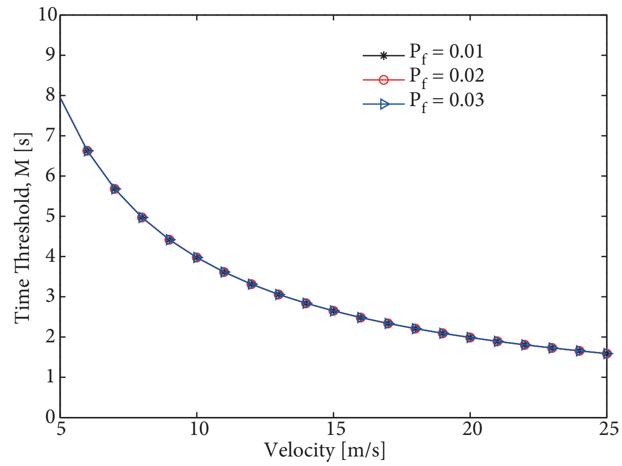

Figure 5. Time threshold versus velocity of the MN.

responds to the velocity of the mobile node. In Figure 6, we depict the impact of the probability of handover failure on M; it can be observed in the microplot in Figure 6 that as P_f increases the value of M varies as well, although very slowly. M adapts to varying values of velocity as well as P_f, though the impact of velocity overshadows the impact of P_f.

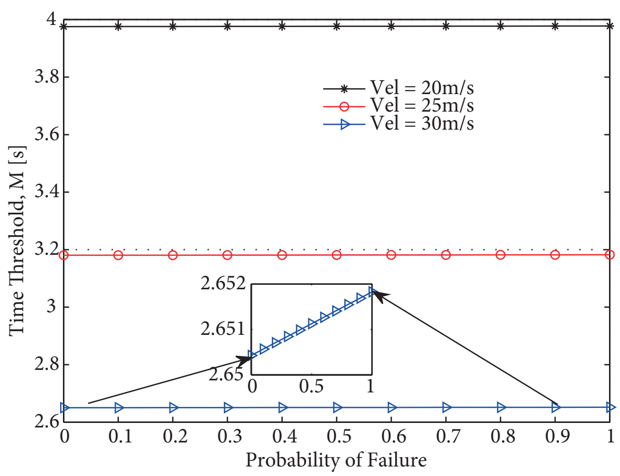

Figure 6. Time threshold versus P_f.

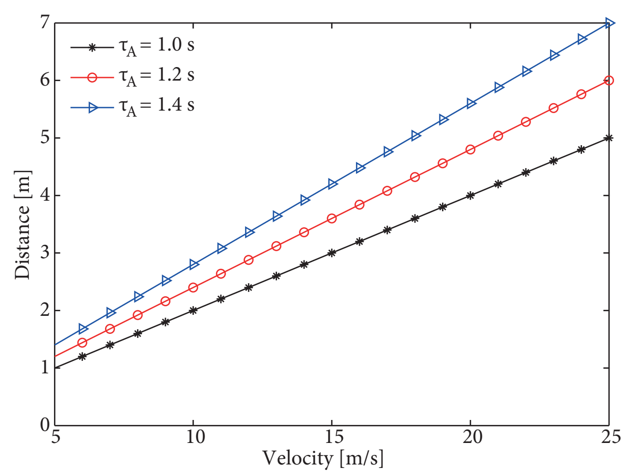

Figure 7. Distance versus velocity of the MN.

It is desirable to minimize the handover latency of the MN into the WLAN cell in order to maximize the utility of the WLAN access. In Figure 7, we observe the impact of velocity on the distance traveled by the MN at various values of latency of handover into the WLAN cell. At $\tau_A = 1$ s, the overall distance traveled by the MN over the entire velocity range is much smaller than at $\tau_A = 1.2$ s and $\tau_A = 1.4$ s. This implies that for smaller values of latency the MN will be able to initiate a handover within a shorter distance as compared to that at higher values of latency. Table 2 shows root mean square error (RMSE) for the models under consideration. The RMSE is a statistical tool that shows how the models deviate from the predefined benchmark value of 0.01. In both cases, the error for the proposed model of P_f and P_u was minimal.

It is important to evaluate the performance of a model as compared to some predefined benchmark.

Table 2. RMSE values for the models.

Model performance	Yan [2]	Hussain (LA) [1]	Hussain [3]	Proposed scheme
P_u*'s RMSE*	0.01485	0.00626	0.00269	0.00109
P_f*'s RMSE*	0.01184	0.00436	0.00300	0.00062

On this note, we measure the efficiency of our proposed probabilistic model in keeping the failure close to the benchmark value using the Nash–Sutcliffe coefficient[3] [18]. The efficiency of the proposed model for a benchmark of 0.01 was 98.82%.

6. Conclusions

This paper has presented a new model for HNE for a mobile node entering a WLAN coverage area from the cellular network. The proposed geometric-based model for HNE extends and improves on theoretical results from the previous mathematical analysis conducted by several researchers. The resulting model is probabilistic and based on various network parameters, which include the random varying cell radius, the angle of traversal, and the velocity of the MN. This model is unique in the sense that it puts into consideration slow fading (shadowing), making the shape of the coverage region to be irregular rather than circular, which has been neglected by previous researchers.

The models presented were validated by comparing simulated results with works of other researchers under similar conditions. The quality of these simulations qualitatively matched the actual behaviors of mobile node traversing a realistic WLAN cell. To the best of our knowledge, this is the first geometric-based model that considers an amoebic cell structure for simulating the probability of handover. The reported results indicate the efficacy of the model in minimizing P_u and P_f. The vertical handover decision scheme presented in this work can be employed as part of the IEEE 802.21 media-independent handover framework, since it aims to support seamless roaming across a diverse set of wireless access technologies. A possible improvement to the proposed HNE scheme will be to consider the effect of fast fading and also consider a scenario where the WLAN AP is mobile. Our future work will consider the effects of fast fading due to multipath, and consider a nonstatic WLAN AP scenario. Further, the work can be extended to include a scenario where the mobile node changes its direction one or more times within the WLAN coverage area.

References

[1] Hussain R, Malik SA, Abrar S, Riaz RA, Khan SA. Minimizing unnecessary handovers in a heterogeneous network environment. PRZ Elektrotechniczn 2012; 88: 314-318.

[2] Yan X, Mani N, Sekercioglu YA. A traveling distance prediction based method to minimize unnecessary handovers from cellular networks to WLANs. IEEE Commun Lett 2008; 12: 14-16.

[3] Hussain R, Malik SA, Abrar S, Riaz RA, Ahmed H, Khan SA. Vertical handover necessity estimation based on a new dwell time prediction model for minimizing unnecessary handovers to a WLAN cell. Wireless Pers Commun 2013; 71: 1217-1230.

[4] Mohanty SA. New architecture for 3G and WLAN integration and intersystem handover management. Wirel Netw 2006; 12: 733-745.

[3] $E = 1 - \frac{\sum_{v=1}^{N} (Q_m^v - Q_o^v)^2}{\sum_{v=1}^{N} (Q_o^v - \bar{Q}_o)^2}$, where Q_m^v is the modeled data at velocity v, and Q_o^v is the observed data at velocity v.

[5] Chang BJ, Chen JF. Cross-layer-based adaptive vertical handoff with predictive RSS in heterogeneous wireless networks. IEEE T Veh Technol 2008; 57: 3679-3692.

[6] Tamea G, Vegni AM, Inzerilli T, Cusani R. A probability-based vertical handover approach to prevent ping-pong effect. In: 2009 6th International Symposium on Wireless Communication Systems; 7–10 September 2009; Tuscany, Italy. New York, NY, USA: IEEE. pp. 181-185.

[7] Wang L, Zawodniok MJ. Bias and CRB analysis of LoS-based and RSS-based ranging methods. IEEE T Veh Technol 2016; 65: 9085-9097.

[8] Teng Y, Liu M, Song M. Effect of outdated CSI on handover decisions in dense networks. IEEE Commun Lett 2017; 21: 2238-2241.

[9] Wu J, Fan P. A survey on high mobility wireless communications: challenges, opportunities and solutions. IEEE Access 2016; 4: 450-476.

[10] He D, Chi C, Chan S, Chen C, Bu J, Yin M. A simple and robust vertical handoff algorithm for heterogeneous wireless mobile networks. Wireless Pers Commun 2011; 59: 361-373.

[11] Liu M, Li Z, Guo X, Dutkiewicz E. Performance analysis and optimization of handoff algorithms in heterogeneous wireless networks. IEEE T Mobile Comput 2008; 7: 846-857.

[12] Jafari AH, Shahhoseini HS. A location aware history-based approach for network selection in heterogeneous wireless networks. Turk J Electr Eng & Comp Sci 2016; 24: 2929-2948.

[13] Zarei M, Ghahfarohi BS, Mahdavi M. Mobility and load aware radio resource management in OFDMA femtocell networks. Turk J Electr Eng & Comp Sci 2017; 25: 1976-1992.

[14] Shanmugam K. A novel candidate network selection based handover management with fuzzy logic in heterogeneous wireless networks. In: 2017 4th International Conference on Advanced Computing and Communication Systems (ICACCS); 6–7 January 2017; Coimbatore, India. New York, NY, USA: IEEE. pp. 1-6.

[15] Rappaport TS. Wireless Communications Principles and Practice. 2nd ed. New York, NY, USA: Prentice Hall PTR, 2002.

[16] Fontan PF, Espineira PM. Modelling the Wireless Propagation Channel: A Simulation Approach with MATLAB. New York, NY, USA: John Wiley and Sons Ltd, 2008.

[17] Papoulis A. Probability, Random Variables, and Stochastic Processes. 3rd ed. New York, NY, USA: McGraw-Hill, 1991.

[18] Yang Q, Chen S, Xie H, Hao X, Zhang W. Application of snowmelt runoff model (SRM) in upper Songhuajiang Basin using MODIS remote sensing data. In: 2016 IEEE International Geoscience and Remote Sensing Symposium (IGARSS); 10–15 July 2016; Beijing, China. New York, NY, USA: IEEE. pp. 4905-4908.